Available online at www.eccomasproceedia.org
Eccomas Proceedia COMPDYN (2017) 3102-3111

ECCOMAS
Proceedia

COMPDYN 2017
6th ECCOMAS Thematic Conference on
Computational Methods in Structural Dynamics and Earthquake Engineering
M. Papadrakakis, M. Fragiadakis (eds.)
Rhodes Island, Greece, 15–17 June 2017

SEISMIC FRAGILITY OF HORIZONTAL PRESSURE VESSELS - EFFECTS OF STRUCTURAL INTERACTION BETWEEN INDUSTRIAL COMPONENTS

J. Korndörfer, B. Hoffmeister and M. Feldmann

Institute of Steel Construction
Mies-van-der-Rohe-Str. 1, 52074 Aachen, Germany
e-mail: korndoerfer@stb.rwth-aachen.de

Keywords: fragility surface, horizontal pressure vessel, cloud analysis, coupled systems, simplified model

Abstract. *The European project "INDUSE-2-SAFETY" aims at the development of a quantitative risk assessment methodology for seismic loss prevention of "special risk" petrochemical plants and components. To demonstrate the capabilities of this approach, a representative case study plant containing standard components is subjected to detailed investigation. Probabilistic seismic demand models are used to establish a relation between seismic demand and structural performance of the components with respect to relevant limit states. The resulting fragility curves are required as an input to the quantitative risk model.*

The case study comprises of a LNG regasification plant which contains various components with extreme variability in structural and dynamic characteristics. Due to process flow related requirements, all of these components are interconnected by an extensive pipe network. In case of an earthquake, these interconnections may cause significant structural interaction effects. The influence of the coupling is hard to predict and thus often neglected or estimated inappropriately in a common structural design of a single plant component. Within this paper, the effects of structural interaction are assessed rigorously for a small part of the LNG plant using finite element methods. The subplant considered for this analysis consists of a horizontal pressure vessel, connected pipes and respective supporting structures.

Twenty-six natural seismic records are selected with respect to uniform site hazard spectra for three different return periods to account for a wide variability of earthquake characteristics such as magnitude, fault distance and wave content are considered in the analysis. Cloud analysis is employed to perform the probabilistic seismic demand analysis which yields the fragility of the horizontal pressure vessel. Besides the variability of the seismic input, the liquid filling level of the vessel as well as the direction of ground motion have been considered as additional sources of uncertainty.

Peer-review under responsibility of the organizing committee of COMPDYN 2017.
doi: 10.7712/120117.5630.18148

1 INTRODUCTION

Industrial plants can be of very complex nature due to a large number of possible components with extreme variability in structural and dynamic characteristics. In addition, process flow related interdependencies between the components govern the plant lay-out including interconnections by pipes and positions of supporting structures. It is, however, common practice to design the structures and components individually; the structural interaction between these subsystems is thus either neglected or taken into account only inappropriately, e.g. by provision of estimated forces without considering deformation compatibilities. These design methods might result in nonconservative assessment of the seismic performance of structures and components resulting in casualties and serious economic losses in case of earthquakes.

The study at hand focusses on the seismic performance of a horizontal pressure vessel, explicitly studying the effect of structural interaction with its surrounding components. The vessel is used for storage of liquefied natural gas (LNG) at an operating pressure of 6 bar. The component has an internal diameter of 2.6 m and a total length of 10.15 m (Volume of 51.2 m^3). It is supported on two steel saddles (one free, one fixed in longitudinal direction) with a spacing of 6.3 m. The thickness of the vessel wall accounts to 8 mm and the material is SA240 Gr. 304 L. The vessel is part of a large LNG plant and is interconnected to several other industrial components by a piping system. For this purpose, two nozzles (DN 450/DN 500) are located on the top side of the vessel. The component under exam together with its surrounding is shown in Figure 1.

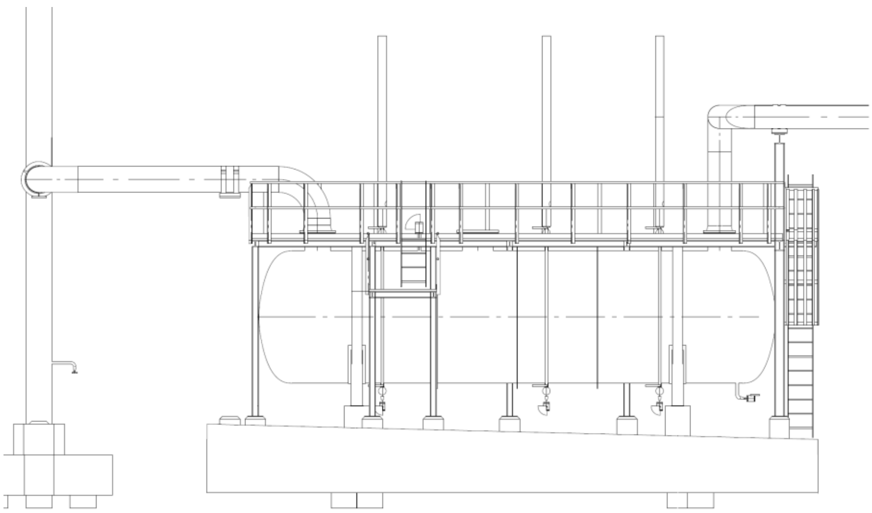

Figure 1: Horizontal pressure vessel under exam together with surrounding pipes and support structures

2 MODELLING APPROACH

2.1 Simplified modelling approach for horizontal pressure vessels

To derive fragilities of a structure numerically, dozens or even hundreds of dynamic transient simulations are required, depending on the probabilistic seismic demand model applied and on the amount of sources of uncertainties considered. Thus, simplified models are required to limit the computational effort and to efficiently assess the influence of different variables towards the fragility of the component under investigation. In the present study, a simplified model with only a few degrees of freedom, as shown in Figure 2, was used and implemented in ANSYS software to approximate the seismic response of the horizontal pressure vessel.

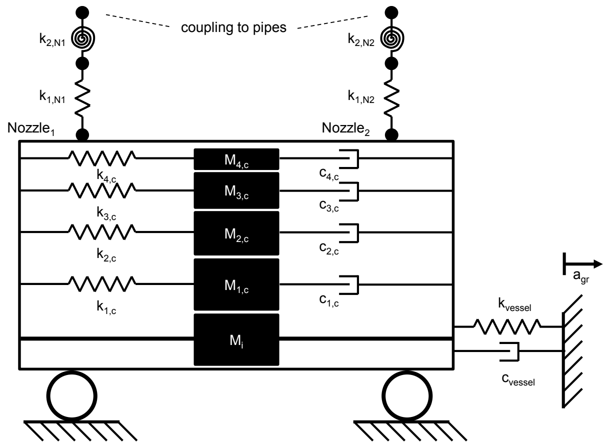

Figure 2: Sketch of the simplified model of the horizontal pressure vessel.

The simplified model is based on the assumption that deformations of the pressure vessel concentrate on the saddle region and the surrounding of the nozzles when subjected to seismic loading. Accordingly, the spring stiffnesses k_{vessel} and $k_{i,Nj}$ have been calibrated to represent the nonlinear deformation behaviour as well as the dynamic structural response of the vessel. Approaches presented by Housner [1] and Karamanos [2] are adopted to take sloshing phenomena into account in a simplified way. The total mass of the pressure vessel is decomposed into an impulsive part (which incorporates the mass of the vessel and the impulsive component of the liquid) and four convective parts to account for the sloshing behaviour of the liquid filling (first four sloshing modes are considered). In the simplified model, the resulting masses are represented as lumped mass elements applied in their respective centre of gravity.

Three different limit states and associated engineering demand parameters (which are used to indicate whether or not the limit states are exceeded) were defined for the fragility analysis on the basis of nonlinear pushover simulations on a rigorous finite element model:

- LS 1: Rupture of vessel wall at saddle location
  (EDP: Base shear)
- LS 2: Rupture of vessel at nozzle transition'
  (EDP: Bending moment at the top of the nozzles)
- LS 3: Failure of the first anchor bolt
  (EDP: Base shear)

For more details on the derivation and verification of the simplified model as well as on the limit state analysis, please refer to [3].

2.2 Subplant model

The simplified model of the pressure vessel has been integrated into a realistic plant environment (coupled model) as indicated in Figure 1. Figure 3 shows the simplified model of the vessel (green) together with the pipes (red) that connect at both nozzle locations. Further, the supporting structure (blue) of the pipes is considered within the subplant.

The support structure consists of steel frames (S235) stiffened by diagonal X and V bracings. The structural elements are modelled using fibre section beam elements (BEAM188) with a bilinear elastic-plastic material behaviour (nominal stiffness/yield strength and 5% kinematic hardening). Additional dead and live loads are considered as nodal masses.

The pipes present in the subplant model are made of stainless steel SA Gr. 304 L which is identical to the material the pressure vessel itself is made of. One of them (DN 500) connects to nozzle 2 and leads to a ventilation stack. While this pipe is considered empty, the other three pipes are assumed to be filled with LNG. A DN 450 pipe connects to nozzle 1 of the pressure

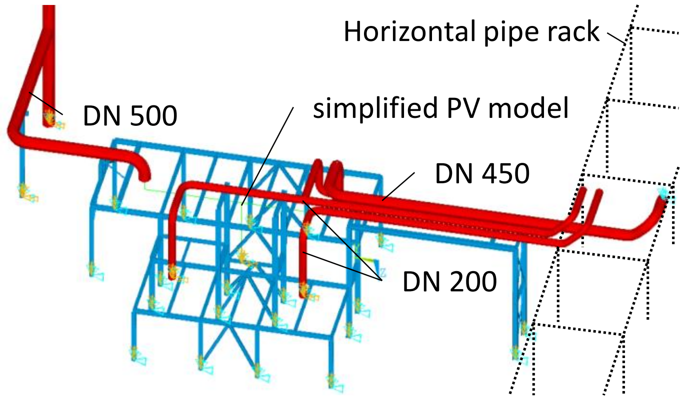

Figure 3: ANSYS model of the simplified pressure vessel model (green) coupled to surrounding pipes (red) and support structure (blue).

vessel whereas two smaller pipes (DN 200) are connected to another component, which is neglected in the model. The pipes continue to a horizontal pipe rack which is not considered in detail. Instead of explicitly modelling the pipe rack and the remaining components of the plant that are interacting with it, the dynamic characteristics of the surrounding of the subplant are taken into account as adjusted boundary conditions. For this in a first step, a modal analysis of the horizontal pipe rack was conducted to determine the decisive Eigenfrequencies of the structure and to estimate the participating masses in the respective modes. Then, single degree of freedom oscillators were employed in both horizontal directions and coupled to the end of the pipes to incorporate the dynamic response of the horizontal pipe rack. By following this approach, only the dominant modes in both directions are considered, while higher modes with low participation factors are neglected for simplicity reasons. The pipes were represented by pipe elements (PIPE288) with a bilinear elastic-plastic material behaviour (E=200000 N/mm²; f_y=200 N/mm²; E_{hard}=0.05·E).

3 FRAGILITY ANALYSIS

3.1 Fragility model

Within this study, fragility is defined with regards to seismic demands only. Thus, resulting fragilities represent the probability of exceeding a specific limit state at a specific level seismic intensity measure (IM) without considering uncertainties in the capacity of the system [4]:

$$F_{Rd}(x) = P[D \geq d^{LS} \mid IM = x] \tag{1}$$

where D describes the seismic demand in terms of a suitable engineering demand parameter (e.g. base shear force, interstorey drift,…) and d^{LS} represents the respective threshold value for the specific engineering demand parameter where the limit state is exceeded. Since uncertainties in the capacity of the system are not considered in a probabilistic manner, d^{LS} is of deterministic nature. On the other hand, the seismic input is considered as a random variable, which means that the obtained seismic demand parameter D is randomly distributed as well.

In a first step, the relation between seismic intensity measure (in the paper at hand, PGA has been adopted) and the seismic engineering demand parameter is established. The functional relationship between conditional median of the demand parameter m_d and the seismic intensity measure IM (probabilistic seismic demand model = PSDM) is generally assumed to follow a power law:

$$m_d = a(IM)^b \tag{2}$$

where a and b are regression parameters that are determined by a linear regression of the $ln(d_i)$ (maximum EDP value observed during a seismic event) over $ln(IM_i)$ values (the index i refers to the i-th seismic event), resulting from the probabilistic seismic demand analysis (e.g. incremental dynamic analysis or cloud analysis). The conditional logarithmic standard deviation of the fitted functional relationship between m_d and IM is calculated using eq. (3).

$$\beta_{d|IM} = \sqrt{\frac{\sum_{i=1}^{n}[ln(d_i) - ln(a(IM_i)^b)]^2}{n - df}} \tag{3}$$

where n is the number of ground motions selected for the probabilistic seismic demand analysis and df is the number of variables estimated in the linear regression (here, 2 variables are estimated – a and b, see equation (2)). Finally, the median m_{Rd} as well as the dispersion β_{Rd} of the demand fragility are calculated using the following equations:

$$m_{Rd} = \left(\frac{d^{LS}}{a}\right)^{1/b} \tag{4}$$

$$\beta_{Rd} = \frac{1}{b}\beta_{d|IM} \tag{5}$$

The seismic fragility is then expressed using a lognormal cumulative distribution function:

$$F_{Rd}(x) = P[D \geq d^{LS}|IM = x] = \Phi\left[\frac{\ln(x/m_{Rd})}{\beta_{Rd}}\right] \tag{6}$$

3.2 Probabilistic seismic demand model

Different methodologies for the probabilistic seismic demand analysis (PSDA) have been presented in literature [5]-[9]. The models most commonly used are the incremental dynamic analysis, the stripe analysis and the cloud analysis. In the present study, cloud analysis was selected for two reasons: Firstly, cloud analysis utilises the "bin" approach - instead of scaling up a single set of accelerograms to increase the intensity measure (which may not be realistic for higher scale factors), multiple sets of slightly scaled natural seismic records are used that have different characteristics (magnitude, fault distance, frequency content). Secondly, less records are usually needed in comparison to the incremental dynamic analysis approach to generate reasonable results. With respect to the computational resources required for transient analyses of the subplant, this is considered a decisive advantage. However, the assumption that the functional relationship between engineering demand parameter and seismic intensity measure follows a power law is not implicitly accurate. While good agreement is generally achieved for the range of intensities considered in the ground motion bins, the validity of results decreases when extrapolating equation (2) to higher intensities.

Within the project INDUSE-2-SAFETY, uniform hazard spectra with different target rates of exceedance for the location of the plant (soil class B) have been derived. Appropriate natural seismic records were selected from the PEER ground motion database and scaled to minimise

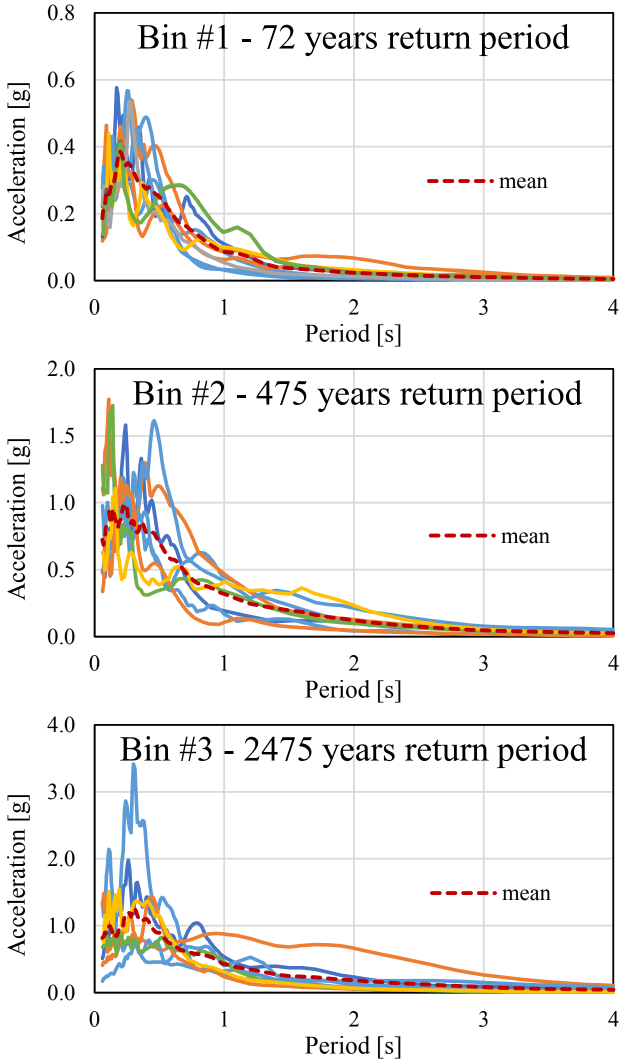

Figure 4: Spectra of seismic record selection

the deviation of mean spectral acceleration and uniform hazard spectra [10]. Three bins have been defined with return periods of 72, 475 and 2475 years. The spectra of the selected accelerograms are depicted in Figure 4. In total, 26 records are used for the PSDA. Bin #1 contains ten different accelerograms while bin #2 and bin #3 encompasses eight records, respectively.

The PSDA has been performed varying coupling conditions of the vessel (uncoupled/coupled), filling levels H and directions of ground excitation α. For the numerical simulations, structural damping was set to 2%, while sloshing modes were damped with 0.5% critical damping.

3.3 Fragility surfaces

In the following, the seismic fragility of the horizontal pressure vessel under investigation is illustrated. For each scenario (filling level H, direction of ground excitation α and coupling condition), the full set of seismic records has been applied and a fragility curve has been derived using cloud method as described earlier. In total, 34 scenarios have been defined which results in 34 fragility curves for each limit state and requires almost 900 transient simulations. To visualize the results (especially the influence of the filling level and the direction of ground motion), multiple fragility curves are merged into fragility surfaces that represent the probability of exceedance of a limit state for a certain level of PGA. For example, the surfaces shown in Figure 5 illustrate the probability of exceeding the limit state 'rupture of vessel at saddle location' for the uncoupled vessel (without considering the surrounding of the pressure vessel). The six surfaces represent different levels of PGA (starting at 0.6 g with incremental increase of 0.4 g in this case).

Obviously, the fragility of the vessel with respect to 'rupture of vessel wall at saddle location' depends significantly on the filling level H (0 corresponds to an empty vessel) and the direction of ground excitation α (0° corresponds to seismic excitation in transversal direction). Generally, the fragility increases with increasing filling level and angle of ground excitation. Seismic loading in longitudinal direction (α = 90°) seems to be more crucial than in axial direction. Comparing the fragility surfaces of the uncoupled vessel (Figure 5) with the coupled situation (Figure 6), probabilities of 'rupture of vessel wall at saddle location' are lower for most situations. Moreover, in the coupled scenario, the influence of the filling level seems to be negligible.

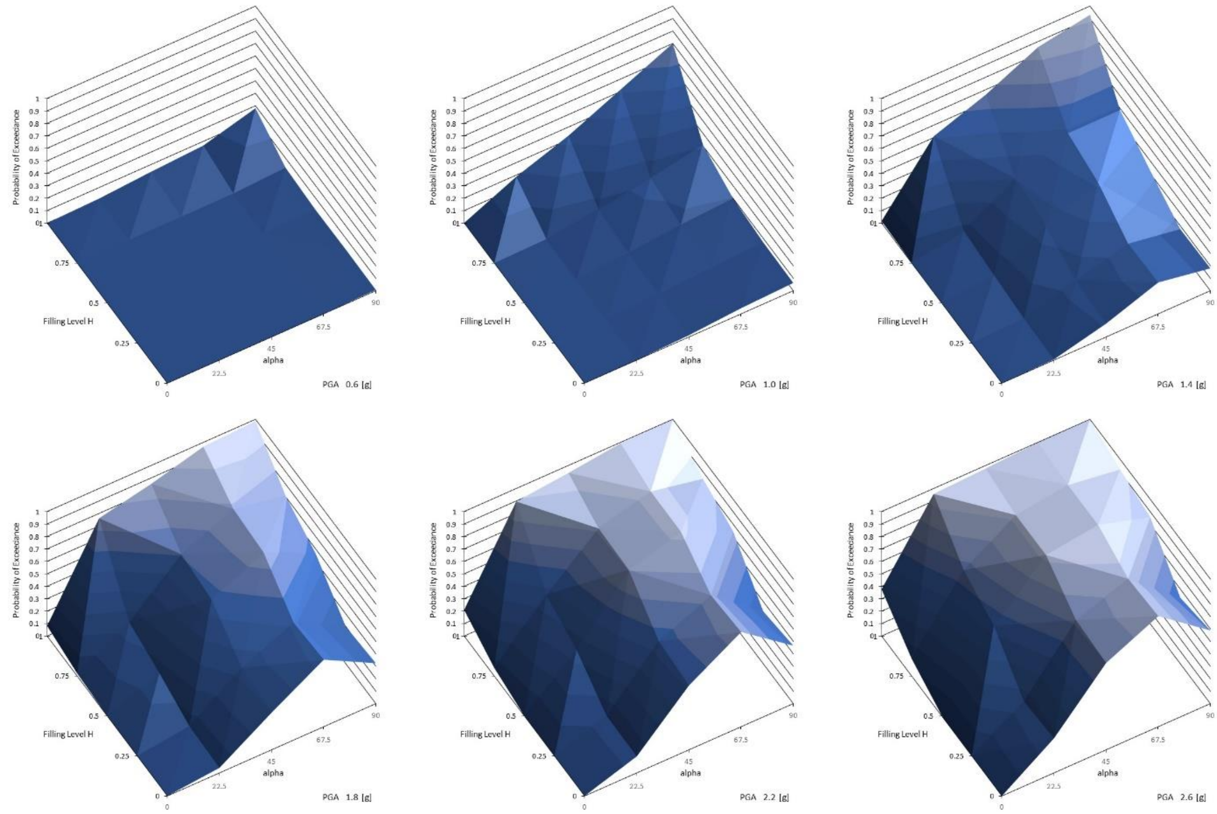

Figure 5: Fragility surface for LS ‘rupture of vessel wall at saddle location’, uncoupled state.

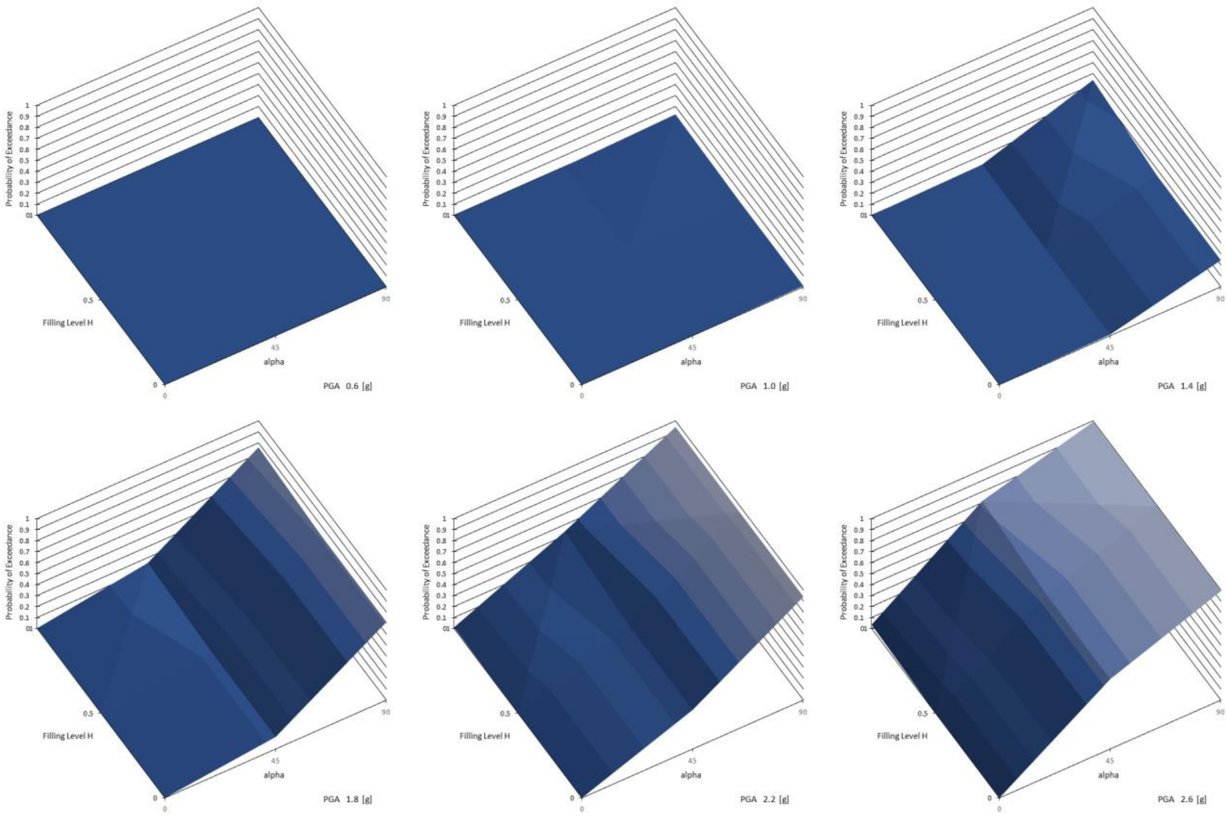

Figure 6: Fragility surface for LS ‘rupture of vessel wall at saddle location’, coupled state.

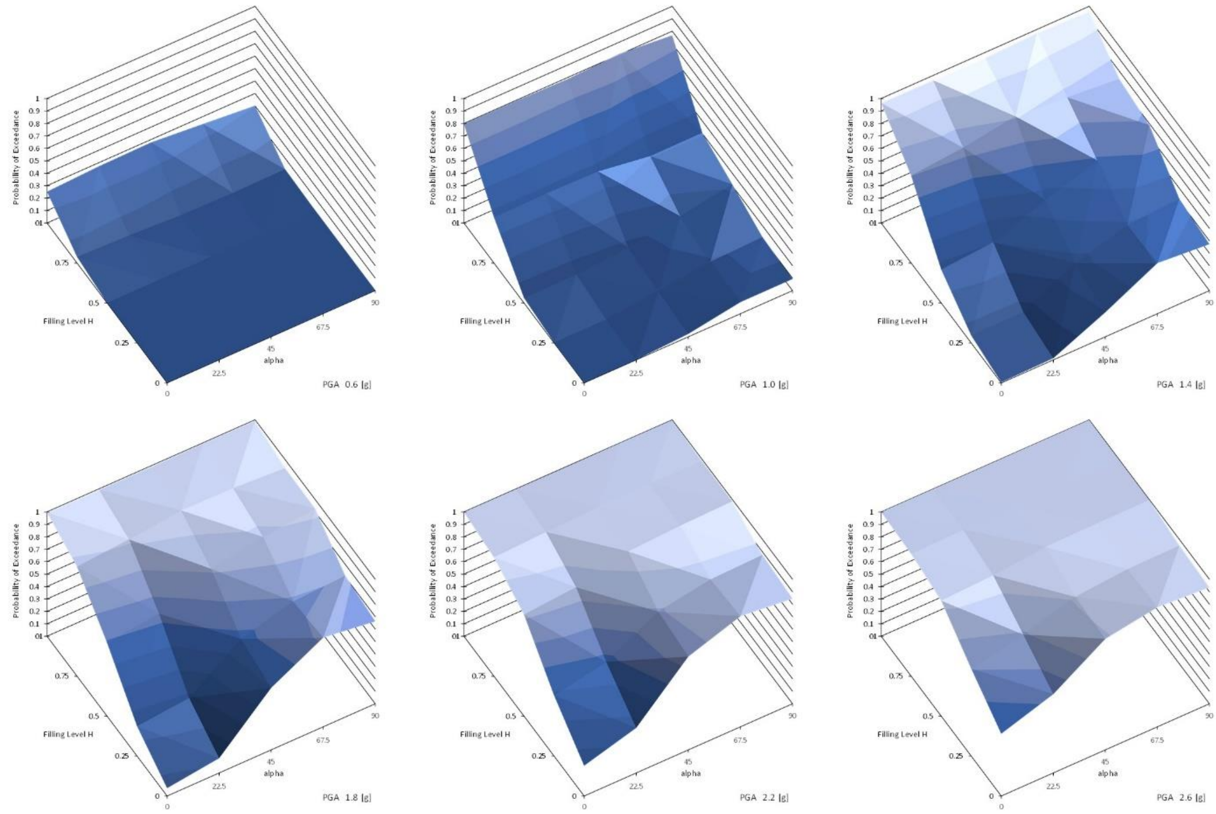

Figure 7: Fragility surface for LS ‘anchor bolt failure’, uncoupled state.

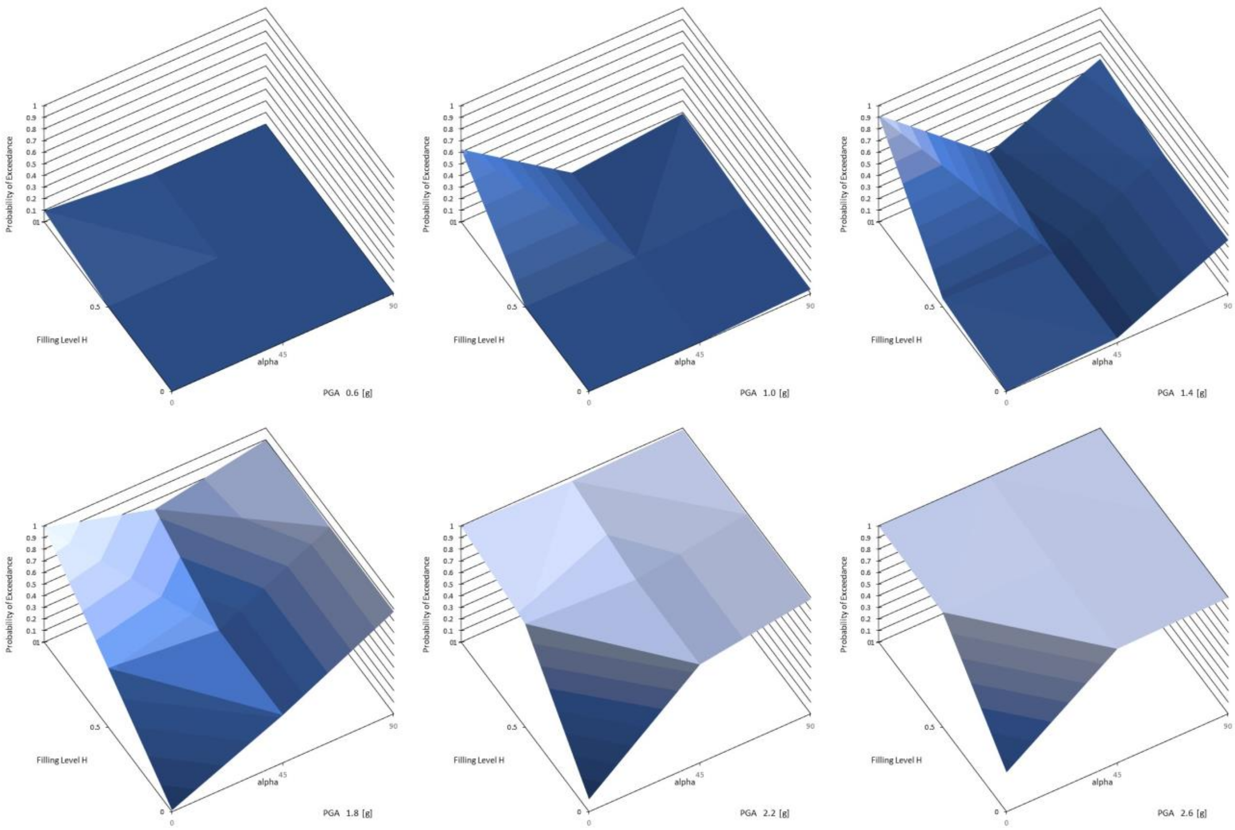

Figure 8: Fragility surface for LS ‘anchor bolt failure’, uncoupled state.

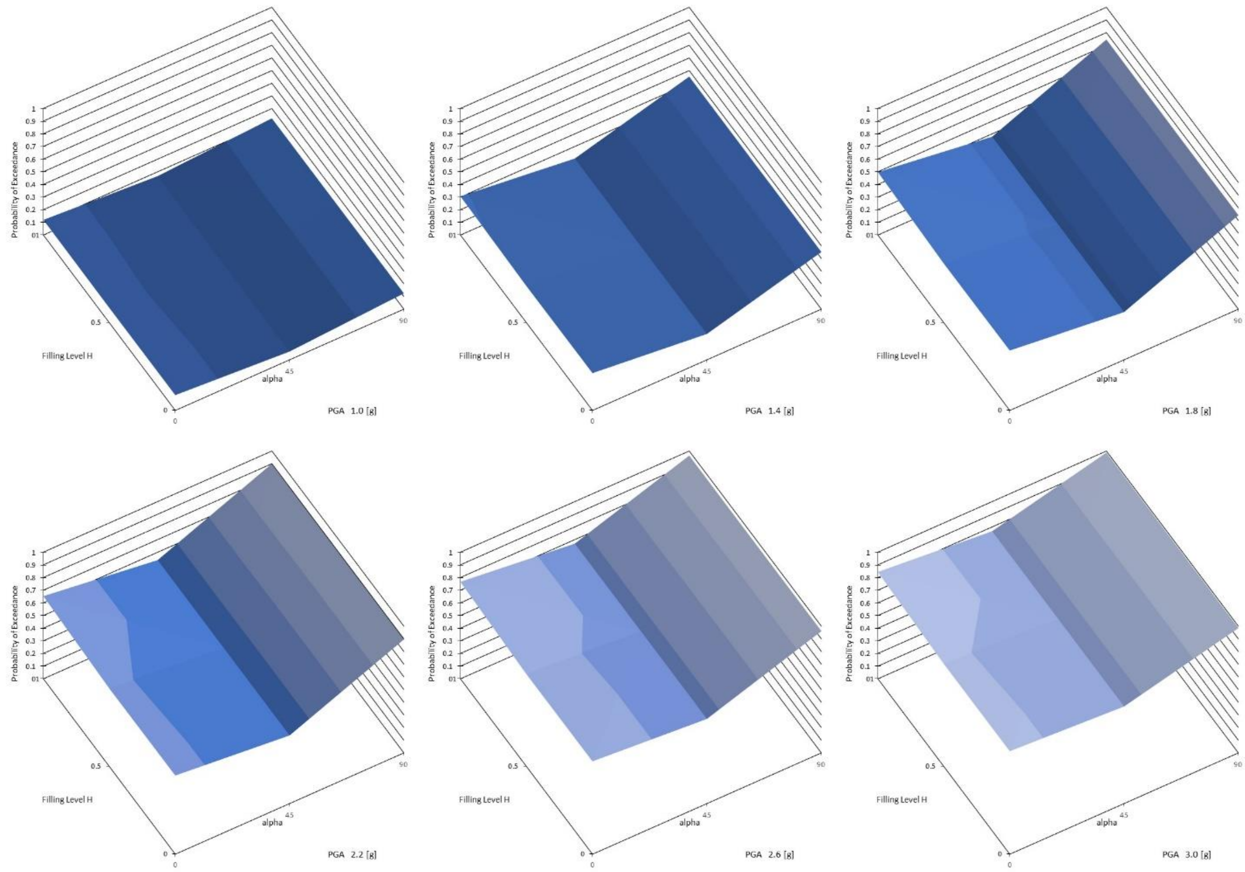

Figure 9: Fragility surface for LS 'rupture at nozzle transition', coupled state.

Figure 7 and Figure 8 depict fragility surfaces for the 'anchor bolt failure' limit state with and without considering the surrounding of the vessel. As already observed for the LS 'rupture of vessel wall at saddle location', the probability of failure decreases in case the coupling is accounted for properly. Independently of the coupling situation, the probability of exceeding 'anchor bolt failure' seems to be higher than exceeding the LS 'rupture of vessel wall at saddle location' (see Figure 5 and Figure 6). However, the fragility in the context of 'anchor bolt failure' can be easily reduced by replacing the existing bolts by higher strength/diameter ones.

Finally, fragility surfaces for the limit state 'rupture at nozzle transition' are shown in Figure 9. This limit state is only relevant for coupled scenarios, since the nozzles are free of load when not coupled to the surrounding piping system. Furthermore, only one of the nozzles (DN 450) is vulnerable to this limit state – the second nozzle has a higher resistance to this failure mode and is at the same time subjected to much lower bending moments. However, even the probability of exceeding the LS 'rupture at nozzle transition' at the DN 450 nozzle seems to be quite low compared to the exceedance of the other two limit states (consider the different level of PGA the surfaces are referencing to). Another observation is that the exceedance of this limit state does not depend on the filling level at all.

4 CONCLUSIONS

Within this study, a horizontal pressure vessel was investigated with respect to its seismic fragility varying the direction of seismic excitation and the filling level. Furthermore, special attention was given to the influence of the boundary conditions, by taking into account the surrounding of the vessel (piping system and support structure). To allow for extensive PSDA, a simplified pressure vessel model, introduced in [3], was adopted for this study. Multiple fragility curves have been merged into fragility surfaces to illustrate the influence of the considered variables on the resulting fragility of the pressure vessel.

Three different limit states have been considered within this study, with ‘anchor bolt failure’ being the one with the highest probability of exceedance for most scenarios. It has also been shown that the probability of exceeding the two limit states ‘anchor bolt failure’ and ‘rupture of vessel wall at saddle location’ is significantly lower when the surrounding of the pressure vessel is taken into account properly. For the vessel, studied within this paper, ‘rupture at nozzle transition’ due to seismic loading has a very low probability of occurrence. However, it is expected that the probability of exceeding this limit state strongly depends on the layout of the coupled piping system.

5 ACKNOWLEDGEMENT

The work presented here is carried out as a research project by different European partners with a financial grant from the Research Fund for Coal and Steel (RFCS) of the European Community. The authors gratefully acknowledge the financial support.

REFERENCES

[1] Housner, Dynamic Pressures on Accelerated Fluid Containers, *Bulletin of the seismological society of America*, 1955.

[2] Karamanos et al., Sloshing Effects on the Seismic Design of Horizontal-Cylindrical and Spherical Industrial Vessels, *Journal of Pressure Vessel Technology*, Vol. 128, pp. 328 – 340, 2005.

[3] Korndörfer et al., Fragility Analysis of Horizontal Pressure Vessels in the Coupled and Uncoupled Case, *Proceedings of the ASME 2016 PVP Conference*, Vancouver, 2016.

[4] Lu et al., Analytical Formulations of Fragility Functions with Applications to Probabilistic Seismic Risk Analysis, *Proceedings to the WCEE 15*, Lisboa, 2012.

[5] Cornell, Jalayer, Hamburger, Foutch, Probabilistic basis for 2000 SAC federal emergency management agency steel moment frame guidelines, *ASCE J. Struct. Eng.*, Vol. 128, No. 4, pp. 526 – 33, 2002.

[6] Jalayer, Direct Probabilistic Seismic Anaysis: Implementing Non-linear Dynamic Assessments. Ph.D. dissertation, Dept. of Civil and Environmental Engineering, Stanford Univ., Stanford, CA, 2003.

[7] Jalayer, Cornell, Alternative non-linear demand estimation methods for probability-based seismic assessments, *Earthquake Engr. & Struct. Dynamics. J.*, Vol. 38, No. 8, pp. 951 – 972, 2009.

[8] Vamvatsikos, Cornell, Incremental Dynamic Analysis, *Earthquake Engr. & Struct. Dynamics. J.*, Vol. 31, No. 3, pp. 291 – 514, 2001.

[9] Mackie, Stojadinović, Comparison of Incremental Dynamic, Cloud and Stripe Methods for Computing Probabilistic Seismic Demand Models, *Proceeding to Structures Congress 2005*, p. 1 – 11, New York, 2005.

[10] Paolacci et al., Component fragility evaluation, seismic safety assessment and design of petrochemical plants under design-basis and beyond-design-basis accident conditions, *Deliverable 1.2*, INDUSE-2-SAFETY project, RFCS, 2015.